BER Performance of Dual Predetection EGC in Correlative Nakagami-m Fading

George K. Karagiannidis, *Member, IEEE*, Dimitris A. Zogas, *Student Member, IEEE*, and Stavros A. Kotsopoulos

***Abstract*—In this letter, an approach to the evaluation of the error performance in dual predetection equal-gain combining (EGC) systems over correlated Nakagami-m fading channels is presented. Deriving an infinite series representation for the characteristic function of the sum of two correlated Nakagami-m variables, a closed-form formula is extracted for binary phase-shift keying and coherent binary frequency-shift keying, while several other modulation schemes are studied, capitalizing on a Parsevals's theorem-based approach, previously published. Numerical results and simulations are also presented to illustrate the proposed mathematical analysis and to point out the effect of the input signal-to-noise ratio unbalancing, the fading severity, and the fading correlation on the system's error performance.**

***Index Terms*—Correlated fading, diversity, equal-gain combiners (EGCs), Nakagami-m fading channels.**

I. Introduction

SIGNALS FROM multiple antennas, or "spatial diversity," can be used to reduce the effects of fading in wireless communications systems and to improve received signal strength. The most popular linear diversity techniques are selection combining (SC), equal-gain combining (EGC), and maximal-ratio combining (MRC). Among these types of diversity combining, EGC provides an intermediate solution as far as the performance and the implementation complexity are concerned. The performance analysis of predetection EGC, assuming independent channel fading, has been studied extensively in the literature. A comprehensive summary with most of the related work is included in [1]. However, independent fading assumes antenna elements be placed sufficiently apart, which is not always realized in practice due to insufficient antenna spacing, when diversity is applied in compact terminals. In this kind of terminal, the fading among the channels is correlated, resulting in a degradation of the diversity gain obtained. Therefore, it is important to understand how the correlation between received signals affects the offered diversity gain. From reviewing the literature, there are few approaches for the performance evaluation of predetection EGC over correlated fading channels. In [2], a formula for the error probability of EGC with orthogonal binary frequency-shift keying (BFSK) operating in correlative Rician time-selective fading is proposed. Recently, Mallik *et al.* in [3] presented a useful approach to the performance analysis for coherent detection of binary signals with dual EGC over correlated Rayleigh channels.

In this letter, extracting an infinite series representation for the characteristic function (CHF) of the sum of two correlated Nakagami-m variables, the error performance of dual predetection EGC systems over correlated Nakagami-m fading channels is studied. More specifically, a closed-form formula is presented for binary phase-shift keying (BPSK) and coherent BFSK, while several other modulation schemes, such as quadrature phase-shift keying (QPSK), M-ary quadrature amplitude modulation (M-QAM), binary differential phase-shift keying (DPSK), and noncoherent BFSK, are studied using the Annamalai *et al.* [4] approach, where the average error-rate integral is transformed into the frequency domain using the Parseval's theorem. Simulations are performed to check the accuracy of the proposed mathematical analysis. The effect of the input signal-to-noise ratio (SNR) imbalance, as well as the fading correlation and the fading severity on the average error probability, is pointed out.

The remainder of this letter is organized as follows. In Section II, a broad range of modulation schemes employing dual EGC are studied. Simulations and numerical results are presented in Section III to illustrate the proposed mathematical analysis. Finally, some concluding remarks are offered in Section IV.

II. Average Error Analysis

In a dual predetection EGC system, the instantaneous output SNR is $\gamma = a^2$, where a is given by [1, eq. (9.46)]

$$a = \sqrt{\frac{E_s}{2N_0}}(a_1 + a_2) \tag{1}$$

with a_1, a_2 being the correlated Nakagami-m envelopes of the input signals [5], E_s is the energy per symbol, and N_0 is the additive white Gaussian noise (AWGN) power spectral density (PSD), assumed equal for both branches. The joint probability density function (PDF) of a_1, a_2 is [5]

$$f_{a_1,a_2}(a_1,a_2) = \frac{4(a_1a_2)^m e^{-\frac{\Omega_2 a_1^2 + \Omega_1 a_2^2}{\Omega_1\Omega_2(1-\rho)}}}{\Gamma(m)\Omega_1\Omega_2(1-\rho)(\sqrt{\rho\Omega_1\Omega_2})^{m-1}} \times I_{m-1}\left(\frac{2\sqrt{\rho}a_1a_2}{\sqrt{\Omega_1\Omega_2}(1-\rho)}\right) \tag{2}$$

with $\Gamma(\cdot)$ being the Gamma function, $I_v(\cdot)$ being the first kind and vth-order modified Bessel function, $\Omega_i = \overline{a_i^2}/m$ with $\overline{a_i^2}$ being the average signal power at the ith branch, m is a parameter describing the fading severity, and ρ is the correlation coefficient between the two short-term powers defined as

$$\rho = \frac{\operatorname{cov}\left(a_1^2, a_2^2\right)}{\sqrt{\operatorname{var}\left(a_1^2\right)\operatorname{var}\left(a_2^2\right)}}, \quad 0 \le \rho < 1. \tag{3}$$

Paper approved by V. A. Aalo, the Editor for Diversity and Fading Channel Theory of the IEEE Communications Society. Manuscript received November 4, 2002; revised May 7, 2003; July 7, 2003; and July 9, 2003.

G. K. Karagiannidis is with the Institute of Space Applications and Remote Sensing, Athens 15236, Greece (e-mail: gkarag@space.noa.gr).

D. A. Zogas and S. A. Kotsopoulos are with the Wireless Telecommunications Laboratory, Department of Electrical and Computer Engineering, University of Patras, Patras 26110, Greece (e-mail: zogas@space.noa.gr; kotsop@ee.upatras.gr).

Digital Object Identifier 10.1109/TCOMM.2003.822166

The CHF of a_1, a_2 is, by definition [6]

$$\Phi_{a_1,a_2}(s_1,s_2)=\int_0^\infty\int_0^\infty f_{a_1,a_2}(a_1,a_2)e^{-js_1a_1-js_2a_2}da_1da_2 \tag{4}$$

where $\sqrt{j}=-1$ and the CHF of a_1+a_2 is given by [6]

$$\Phi_{a_1+a_2}(s)=\int_0^\infty\int_0^\infty f_{a_1,a_2}(a_1,a_2)e^{-js(a_1+a_2)}da_1da_2. \tag{5}$$

Substituting (2) in (5) and using the infinite series representation for the Bessel function [7, eq. (9.6.10)], the CHF of a_1+a_2 can be written as

$$\begin{aligned}\Phi_{a_1+a_2}(s)=&\frac{4(1-\rho)^{-m}}{\Gamma(m)(\Omega_1\Omega_2)^m}\sum_{k=0}^{\infty}\frac{1}{k!\Gamma(m+k)}\\&\times\left(\frac{\sqrt{\rho}}{\sqrt{\Omega_1\Omega_2}(1-\rho)}\right)^{2k}\\&\times\int_0^\infty a_1^{2m+2k-1}e^{-jsa_1-\frac{a_1^2}{\Omega_1(1-\rho)}}da_1\\&\times\int_0^\infty a_2^{2m+2k-1}e^{-jsa_2-\frac{a_2^2}{\Omega_2(1-\rho)}}da_2.\end{aligned} \tag{6}$$

The integrals in (6) can be expressed in terms of the parabolic cylinder function using [8, eq. (3.462/1)], which gives

$$\begin{aligned}\Phi_{a_1+a_2}(s)=&\frac{(1-\rho)^m}{2^{2m-2}\Gamma(m)}\sum_{k=0}^{\infty}\frac{2^{-2k}\rho^k\left[\Gamma(2m+2k)\right]^2}{k!\Gamma(m+k)}\\&\times e^{\frac{s^2(1-\rho)}{8}(\Omega_1+\Omega_2)}\\&\times D_{-(2m+2k)}\left(\frac{js\sqrt{\Omega_1(1-\rho)}}{\sqrt{2}}\right)\\&\times D_{-(2m+2k)}\left(\frac{js\sqrt{\Omega_2(1-\rho)}}{\sqrt{2}}\right)\end{aligned} \tag{7}$$

where $D_{-v}(z)$ is the parabolic cylinder function of order v and argument z. Finally, using [8, eq. (9.240)] and [7, eq. (6.118)] and after some algebraic manipulations, the CHF of a_1+a_2 can be restated in terms of the more familiar confluent hypergeometric function of the first kind ${}_1F_1(\cdot;\cdot;\cdot)$ [8, eq. (9.210)] as

$$\Phi_{a_1+a_2}(s)=\frac{(1-\rho)^m}{\Gamma(m)}\sum_{k=0}^{\infty}\frac{\rho^k}{k!\Gamma(m+k)}A(\Omega_1)A(\Omega_2) \tag{8}$$

with

$$\begin{aligned}A(x)=&\Gamma(m+k){}_1F_1\left(m+k;\frac{1}{2};-\frac{x(1-\rho)}{4}s^2\right)\\&+js\sqrt{x(1-\rho)}\Gamma\left(m+k+\frac{1}{2}\right)\\&\times{}_1F_1\left(m+k+\frac{1}{2};\frac{3}{2};-\frac{x(1-\rho)}{4}s^2\right).\end{aligned} \tag{9}$$

Taking into account that $\Phi_a(s)=\Phi_{a_1+a_2}(\sqrt{E_s/2N_0}s)$ [6] and that the input average SNRs are $\bar{\gamma}_i=\overline{a_i^2}(E_s/N_0)=m\Omega_i(E_s/N_0)$, the CHF of a can be finally written as

$$\Phi_a(s)=\frac{(1-\rho)^m}{\Gamma(m)}\sum_{k=0}^{\infty}\frac{\rho^k}{k!\Gamma(m+k)}A\left(\frac{\bar{\gamma}_1}{2m}\right)A\left(\frac{\bar{\gamma}_2}{2m}\right). \tag{10}$$

A. DPSK, Noncoherent BFSK, Multilevel Signaling (M-PSK, M-QAM)

Using the Parseval's theorem approach, presented in [4], the average symbol-error probability (ASEP) can be evaluated for several coherent and noncoherent modulation schemes as

$$P_s=\frac{1}{\pi}\int_0^\infty\Re\left\{G^*(s)\Phi_a(s)\right\}ds \tag{11}$$

where the notation $\Re\{\cdot\}$ denotes the real-part operator and $G^*(s)$ the complex conjugate of the Fourier transform of the conditional error probability. For binary DPSK and noncoherent BFSK, $G(s)$ is given by [4, eq. (10)]

$$G(s)=\frac{b_1}{\sqrt{b_2}}\left[\frac{\sqrt{\pi}}{2}e^{-\frac{s^2}{4b_2}}+jF\left(\frac{s}{2\sqrt{b_2}}\right)\right] \tag{12}$$

where $b_1=0.5$, $b_2=1$ for DPSK, $b_1=0.5$, $b_2=0.5$ for BFSK, and $F(\cdot)$ denotes the Dawson's integral

$$F(x)=e^{-x^2}\int_0^x e^{t^2}dt=x_1F_1\left(1;\frac{3}{2};-x^2\right) \tag{13}$$

since for QPSK or M-QAM, $G(\cdot)$ is given by [4, eq. (13)]

$$\begin{aligned}G(s)=&\frac{2b_1}{s\sqrt{\pi}}F\left(\frac{s}{2\sqrt{b_2}}\right)-\frac{4b_3}{s\sqrt{\pi}}\\&\times\left[F\left(\frac{s}{2\sqrt{b_2}}\right)-F\left(\frac{s}{2\sqrt{2b_2}}\right)e^{-\frac{s^2}{8b_2}}\right]\\&+j\left\{\frac{b_1}{s}\left[1-e^{\frac{-s^2}{4b_2}}\right]\right.\\&\left.-\frac{b_3}{s}\left[1-e^{-\frac{s^2}{4b_2}}-\frac{4}{\pi}F^2\left(\frac{s}{2\sqrt{2b_2}}\right)\right]\right\}\end{aligned} \tag{14}$$

where $b_1=1$, $b_2=1/2$, $b_3=1/4$ for QPSK and $b_1=2(1-1/\sqrt{M})$, $b_2=1.5/(M-1)$, $b_3=(1-1/\sqrt{M})^2$ for M-QAM. The corresponding formula for M-PSK is given in [4, eq. (17)] in a more complex form with a definite integral.

Some points about the evaluation of the integral in (11) are necessary to discuss here. Let

$$g(s)=\Re\left\{G^*(s)\Phi(s)\right\}. \tag{15}$$

It can be easily verified that, as $s\to 0$, the limit of $g(s)$ is

$$\lim_{s\to 0}\left[g(s)\right]=\begin{cases}\frac{b_1(1-\rho)^{1-m}}{2\sqrt{b_2\pi}}, & \text{for DPSK, noncoh. BFSK}\\ 0, & \text{for QPSK, } M\text{-QAM}\end{cases} \tag{16}$$

while as $s\to\infty$, it is obvious through observation that $g(s)=0$ for both cases. Hence, if numerical integration is performed, it is only needed to integrate $g(s)$ over a finite interval $[0,u]$. However, although $g(s)$ is continuous in $[0,u]$, it oscillates between peaks and valleys near to zero, making difficult its approximation with a single polynomial, as, e.g., Chebyshev. In this case, it is suitable, instead of using a single polynomial for the whole

range $[0, u]$, to use piecewise Gaussian quadrature numerical integration. Such a technique was used in [9] for the evaluation of the outage probability in cellular systems.

B. BPSK and Coherent BFSK

In the case of coherent binary signaling schemes with EGC, an expression for the ASEP performance is given in [4, eq. (19)]

$$P_s = \frac{1}{2} - \frac{1}{2\pi}\int_0^{\infty} t^{-1}e^{-t}\,\Im\left\{\Phi_\alpha\left(2\sqrt{bt}\right)\right\}dt \qquad (17)$$

where the notation $\Im\{\cdot\}$ denotes the imagine-part operator, $b = 1$ for BPSK, and $b = 0.5$ for coherent BFSK. After some algebraic manipulations, it can be shown that

$$\Im\left\{\Phi_a(2\sqrt{bt})\right\} = \frac{(1-\rho)^{m+\frac{1}{2}}\sqrt{2b}}{\sqrt{m}\Gamma(m)} \times \sum_{k=0}^{\infty}\frac{\rho^k\Gamma\left(m+k+\frac{1}{2}\right)}{k!}\left[G(t,\bar{\gamma}_1,\bar{\gamma}_2)+G(t,\bar{\gamma}_2,\bar{\gamma}_1)\right] \qquad (18)$$

where

$$G(t,x,y) = \sqrt{ty}{}_1F_1\left(m+k;\frac{1}{2};-ctx\right) \times {}_1F_1\left(m+k+\frac{1}{2};\frac{3}{2};-cty\right) \qquad (19)$$

and $c = b(1-\rho)/2m$. Applying Kummer's transformation formula [7, eq. (13.1/27)] for the confluent hypergeometric functions in (18), the integrals produced in (17) have the following form:

$$I = \int_0^{\infty} t^{v-1}e^{-wt}{}_1F_1(u_1;v_1;z_1t){}_1F_1(u_2;v_2;z_2t)dt \qquad (20)$$

and can be solved using [4, App. C]. Finally, combining (17), (18), and (20), we obtain the final expression for the ASEP performance of BPSK and coherent BFSK, given in (21) at the bottom of the page. $F_2(\cdot;\cdot,\cdot;\cdot,\cdot;\cdot,\cdot)$ is the hypergeometric function of two variables [8, Eq. 9.180/2]. A brief study for the rate of convergence of the infinite sum in (21) at the sixth significant figure, is as follows. For $m = 1.8$ and $\bar{\gamma}_1 = \bar{\gamma}_2 = 8$ dB, nine terms are needed for $\rho = 0.2$, 22 for $\rho = 0.5$, 52 for $\rho = 0.7$, and 124 for $\rho = 0.9$.

For $m = 1$, (21) gives the same results as in [3, eq. (15)]. The differences in the final formulas are due to the use of the Hermite representation for ${}_1F_1(\cdot;\cdot;\cdot)$ in [3]. For $\rho = 0$ in (21), only the $k = 0$ term of the summation over k is nonzero, which leads to the same formulation as in [4, eq. (29)].

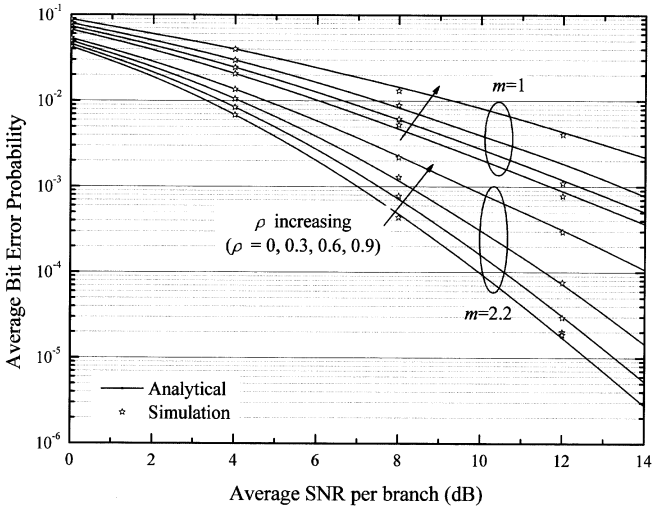

Fig. 1. Error performance of BPSK for $\bar{\gamma}_1 = \bar{\gamma}_2$.

III. Numerical Results and Discussion

Simulations were performed and the results were compared with the corresponding proposed mathematical analysis in order to check the accuracy of the derived formulas. The computer simulation was written in C^{++} programming language, and over 10^7 correlated Nakagami-m fading samples are generated using the algorithm presented in [10]. In order to simulate the error performance, we consider a digital transmitter in which a number of complex symbols are generated, using Gray encoding and then passed through a root raised cosine (RRC) filter, which satisfies the first Nyquist's criterion. Also, it is assumed that the channel corrupts the signal by multiplicative nonselective fading as well as AWGN, having two-sided PSD N_0. At the receiver, assuming perfect channel estimation of the random phases, the output of the EGC combiner is passed through a RRC filter, which is matched to the premodulation filter in the transmitter. The signal is sampled every T_s seconds, where T_s is the duration of the complex symbols.

Figs. 1 and 2 plot the error performance of BPSK employing EGC versus the average SNR per branch, $(\bar{\gamma}_1 + \bar{\gamma}_2)/2$, for equal average SNRs $\bar{\gamma}_1 = \bar{\gamma}_2$, and for unequal branch SNRs $\bar{\gamma}_1 = \bar{\gamma}_2/5$, respectively, and for several values of the parameters m and ρ. Furthermore, Figs. 3 and 4 depict the performance of QPSK and 16-quadrature amplitude modulation (QAM), respectively, for several values of the parameters m and ρ. As it was expected, for a given SNR per branch, the bit-error rate (BER) performance deteriorates with an increase of ρ, while it

$$P_s = \frac{1}{2} - \frac{\sqrt{b}(1-\rho)^{m+\frac{1}{2}}}{\sqrt{2\pi m}\Gamma(m)\left[c(\bar{\gamma}_1+\bar{\gamma}_2)+1\right]^{\frac{1}{2}}}\sum_{k=0}^{\infty}\frac{\rho^k}{k!}\Gamma\left(m+k+\frac{1}{2}\right) \times\left[\sqrt{\bar{\gamma}_2}F_2\left(\frac{1}{2};\frac{1}{2}-m-k,1-m-k;\frac{1}{2},\frac{3}{2};\frac{c\bar{\gamma}_1}{c(\bar{\gamma}_1+\bar{\gamma}_2)+1},\frac{c\bar{\gamma}_2}{c(\bar{\gamma}_1+\bar{\gamma}_2)+1}\right) +\sqrt{\bar{\gamma}_1}F_2\left(\frac{1}{2};1-m-k,\frac{1}{2}-m-k;\frac{3}{2},\frac{1}{2};\frac{c\bar{\gamma}_2}{c(\bar{\gamma}_1+\bar{\gamma}_2)+1},\frac{c\bar{\gamma}_1}{c(\bar{\gamma}_1+\bar{\gamma}_2)+1}\right)\right] \qquad (21)$$

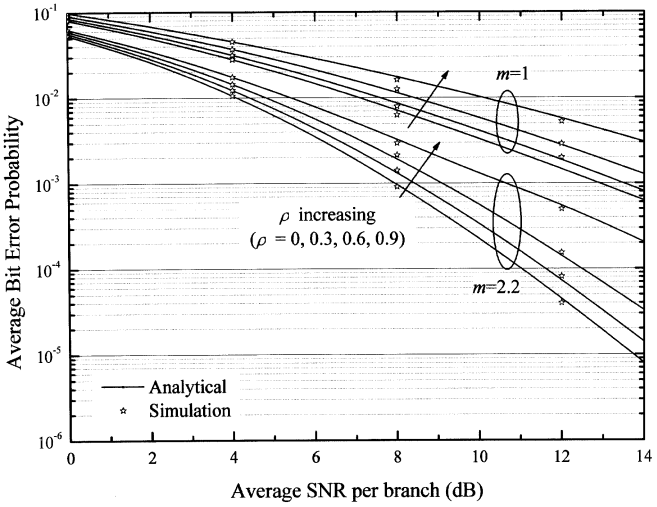

Fig. 2. Error performance of BPSK for $\bar{\gamma}_1 = \bar{\gamma}_2/5$.

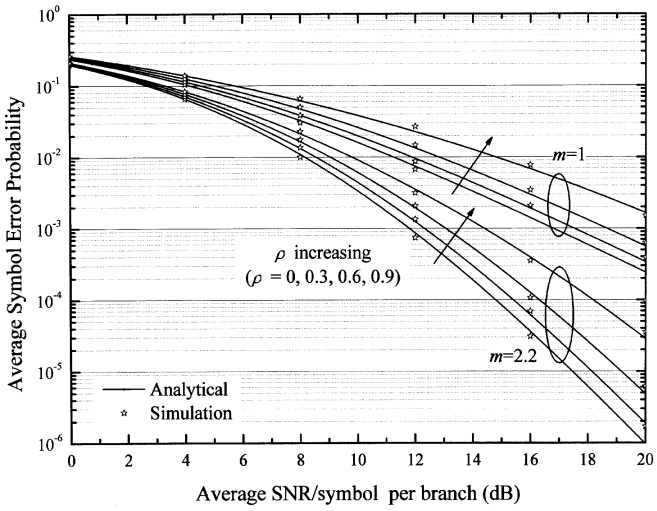

Fig. 3. Error performance of QPSK for $\bar{\gamma}_1 = \bar{\gamma}_2$.

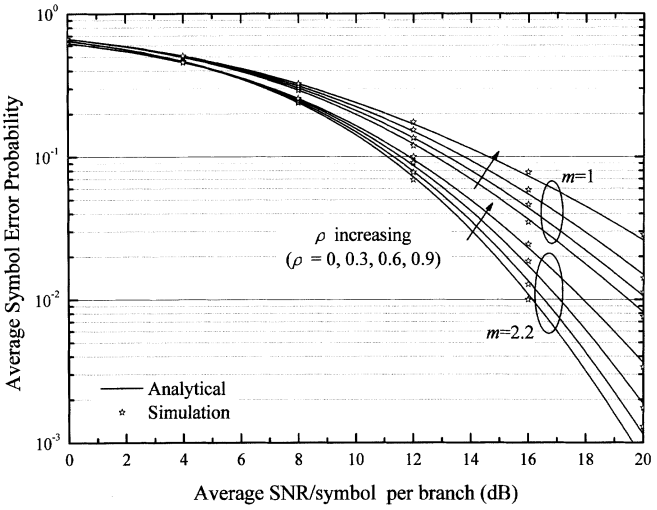

Fig. 4. Error performance of 16-QAM for $\bar{\gamma}_1 = \bar{\gamma}_2$.

improves with an increase of m. Moreover, from Figs. 1 and 2, it is observed that a system with equal branch SNRs performs better than that with unequal branch SNRs, which is to be expected, since in EGC, all the diversity branches are treated equally. Finally, it is evident that the proposed mathematical analysis gives exact results compared with simulations.

IV. Conclusion

In this letter, deriving a useful expression for the CHF of the sum of two correlated Nakagami-m envelopes, an approach to the error performance of a dual predetection EGC system in correlative Nakagami-m fading is presented. A broad class of modulation schemes are studied and numerical results depict clearly the effect of fading correlation, fading severity, and input SNRs unbalancing on the EGC error performance. Simulations show the accuracy of the proposed mathematical analysis.

Just before the time of publication, it came to our attention that other in dependent contributions dealing with the error performance of dual EGC over correlated fading channels have been published [11]–[13]. The material preseented in this letter differs from that of [11] and [12] in the methodology used, since in [13], the analysis is also based on the CHF of the sum of two correlated fading envelopes.

Acknowledgment

The authors would like to thank the anonymous reviewers and the Editor, V. A. Aalo, for their valuable comments that considerably improved the quality of this letter.

References

[1] M. K. Simon and M.-S. Alouini, *Digital Communication Over Fading Channels*, 1st ed. New York: Wiley, 2000.

[2] M. Vitetta, U. Mengali, and D. P. Taylor, "An error probability formula for noncoherent orthogonal binary FSK with dual diversity on correlated Rician channels," *IEEE Commun. Lett.*, pp. 43–45, Feb. 1999.

[3] R. K. Mallik, M. Z. Win, and J. H. Winters, "Performance of dual-diversity EGC in correlated Rayleigh fading with unequal branch SNRs," *IEEE Trans. Commun.*, vol. 50, pp. 1041–1044, July 2002.

[4] A. Annamalai, C. Tellambura, and V. K. Bhargava, "Equal-gain diversity receiver performance in wireless channels," *IEEE Trans. Commun.*, vol. 48, pp. 1732–1745, Oct. 2000.

[5] M. Nakagami, "The m-distribution—a general formula of intensity distribution of rapid fading," in *Statistical Methods in Radio Wave Propagation*, W. G. Hoffman, Ed. Oxford, U.K.: Pergamon, 1960.

[6] A. Papoulis, *Probability, Random Variables, and Stochastic Processes*, 3rd ed. New York: McGraw-Hill, 1991.

[7] M. Abramovitz and I. A. Stegun, *Handbook of Mathematical Functions With Formulas, Graphs, and Mathematical Tables*, 9th ed. New York: Dover, 1972.

[8] I. S. Gradshteyn and I. M. Ryzhik, *Table of Integrals, Series, and Products*, 5th ed. New York: Academic, 1994.

[9] Q. T. Zhang, "Outage probability in cellular mobile radio due to Nakagami signal and interferers with arbitrary parameters," *IEEE Trans. Veh. Technol.*, vol. 45, pp. 364–372, May 1996.

[10] Y.-C. Ko, "Analysis techniques for the performance evaluation of wireless communication systems and estimation of wireless channels," Ph.D. dissertation, Univ. Minnesota, Minneapolis, MN, 2001.

[11] C.-D. Iskander and P. T. Mathiopoulos, "Performance of M-QAM with coherent equal-gain combining in correlated Nakagami-m fading," *Electron. Lett.*, vol. 39, no. 1, pp. 141–142, Jan. 2003.

[12] ——, "Performance of dual-branch coherent equal-gain combining in correlated Nakagami-m fading," *Electron. Lett.*, vol. 39, no. 15, pp. 1152–1154, July 2003.

[13] A. Annamali, V. Ramanathan, and C. Tellambura, "Analysis of equal-gain diversity receiver in correlated fading channels," in *Proc. IEEE Vehicular Technology Conf.*, Birmingham, AL, May 2002, pp. 2038–2041.